

Recognizing the topological charge of orbital angular momentum beams under atmospheric turbulence by linear photodiode array detectors with convolutional neural networks

Jie Xue^{a,b}, Bing Zhu^{*a,b}

^aDepartment of Electronic Engineering and Information Science, University of Science and Technology of China, 96 Jinzhai Road, Hefei, China 230026;

^bKey Laboratory of Electromagnetic Space Information, Chinese Academy of Sciences, 96 Jinzhai Road, Hefei, China 230026

ABSTRACT

We propose a new scheme for recognizing the topological charge (TC) of orbital angular momentum (OAM) beams using convolutional neural networks (CNN) based on the focusing of cylindrical lenses and the detection of linear photodiode arrays (PDAs). Simulations and experiments are conducted. For the superimposed OAM sets with different TC values and different TC intervals, the effects of atmospheric turbulence disturbances on recognition accuracy are explored separately, where the turbulence disturbances to the superimposed OAM beams are measured by the coherence length r_0 . The simulation results show that the recognition accuracy decreases as the turbulence disturbances increase. With 16-unit PDAs, the TC of the superimposed OAM set $l \in \{\pm 1, \pm 2, \pm 3, \pm 4\}$ can be recognized with 100% accuracy under weak (the coherence length $r_0 = 16.16$ cm) and intermediate (the coherence length $r_0 = 10.66$ cm) turbulence disturbances, and above 90% accuracy under a strong (the coherence length $r_0 = 4.06$ cm) turbulence disturbance. In the experiment under weak (the coherence length $r_0 = 13.01$ cm) and intermediate (the coherence length $r_0 = 8.59$ cm) laboratory-simulated turbulence disturbances, with 16-unit PDAs, the recognition accuracy reaches 100% and 99.65%, respectively. The experimental results verify the results of the simulation.

Keywords: orbital angular momentum, atmospheric turbulence, convolutional neural networks, linear photodiode arrays

1. INTRODUCTION

With the infinite topological charges (TCs) and the orthogonality, the orbital angular momentum (OAM) beams show a potential to expand system capacity in communication systems.¹ In free-space optical (FSO) communication systems using OAM beams, the information carried by the OAM beams after transmission under atmospheric turbulence requires efficient extraction at high quality and high speed at the receiver.² The atmospheric turbulence causes optical wavefront distortion,³ which is the main technical bottleneck in OAM-FSO communication.^{1,4} It affects the correct recognition of the TC of OAM beams and leads to an increase in the bit error rate (BER) in OAM-FSO communication.⁵

To effectively recognize the TC of OAM beams under atmospheric turbulence, schemes using machine learning, especially convolutional neural networks (CNN), have been proposed for OAM optical communications.^{6,7,8} In 2014, Krenn *et al.*⁶ used artificial neural networks for the first time to effectively recognize the TC of OAM beams. They performed experiments on the transmission and recognition of OAM beams under the atmospheric channel in Vienna. The images of OAM beams after atmospheric turbulence transmission were captured by an area charge-coupled device (CCD) camera and input to neural networks for recognition. The frame rate of the CCD camera is only 50 Hz. In 2017, Li *et al.*⁷ demonstrated the superiority of CNN in accurately recognizing the TC of OAM beams under atmospheric turbulence. To further improve the TC recognition performance of OAM beams, a CNN-based scheme for joint atmospheric turbulence detection and TC recognition was proposed, where the images of OAM beams after atmospheric turbulence transmission were also captured by a CCD camera.⁸ Despite the excellence in terms of recognition accuracy, the recognition rates are limited by the low framerate at about 50 Hz of the CCDs,^{4,6} which fails to serve the needs of practical OAM-FSO communications. To accelerate the recognition rate, a CNN-based scheme using ring photodetector arrays was proposed,⁹ but found lacking in practicality.

*zbing@ustc.edu.cn

Because superimposed OAM beams have more distinctive characteristics¹⁰ and are less sensitive¹¹ to turbulence, we propose a new scheme to recognize the TC of the superimposed OAM beams based on CNN. Simulation and experimental results verify the feasibility and effectiveness of the proposed scheme, which can achieve TC recognition with both high speed and practicality.

2. SIMULATION

2.1 Principles

The schematic diagram of the proposed scheme is shown in Fig. 1. At the transmitter, a Gaussian beam with a wavelength of 632.8 nm is emitted from a laser and modulated by a spatial light modulator (SLM) to generate a superimposed OAM beam. The superimposed OAM beam propagates through an atmospheric turbulence channel. At the receiver, the beam is focused by two cylindrical lenses and detected by two 16-unit linear photodiode arrays (PDAs). The one-dimensional (1D) signals are then converted into digital signals by analog-to-digital converters. Finally, the data are used as input to CNN for recognizing the TC of the superimposed OAM beams. In the system, the linear PDAs feature the ability to work at high speed.

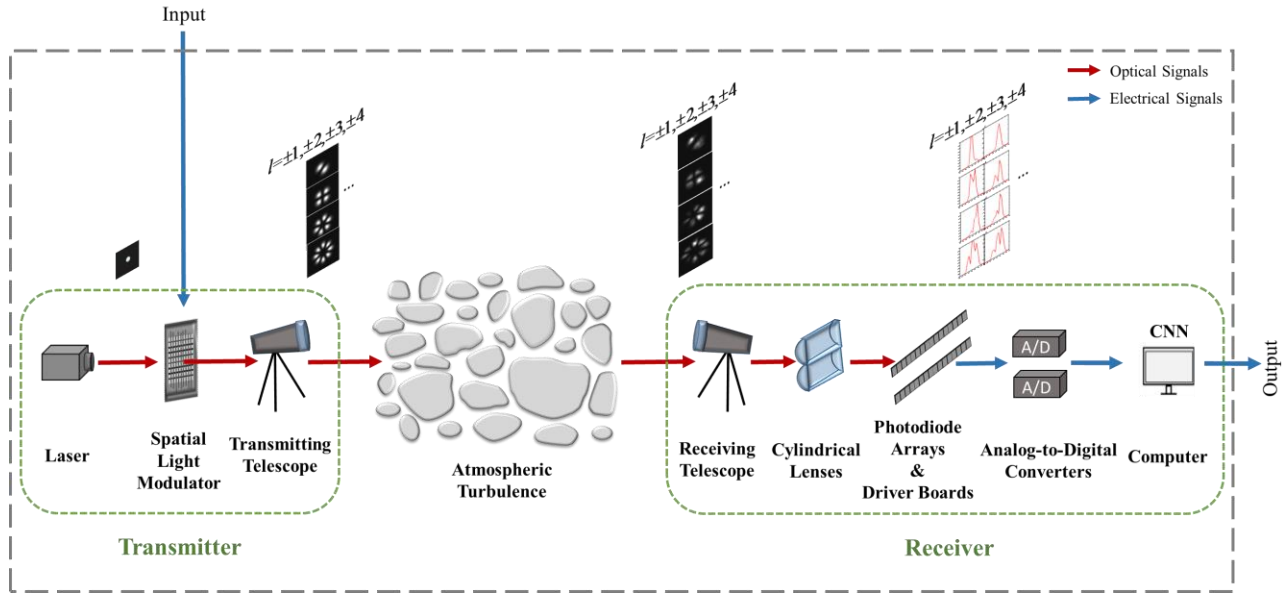


Figure 1. Schematic diagram of the scheme for recognizing the TC of OAM beams under atmospheric turbulence.

We simulate the generation, transmission, and detection of superimposed OAM beams under a 1 km atmospheric turbulence channel.

The optic field of a superimposed OAM beam with a radial mode of 0 can be expressed as¹⁰

$$U_{\pm l}(r, \varphi, z) = \frac{1}{w(z)} \sqrt{\frac{2}{\pi |l|!}} \left(\frac{r\sqrt{2}}{w(z)} \right)^{|l|} \exp\left(\frac{-r^2}{w^2(z)}\right) \exp\left[\frac{ik_0 r^2 z}{2(z^2 + z_R^2)}\right] \exp\left[-i(|l|+1) \tan^{-1}\left(\frac{z}{z_R}\right)\right] \cdot [\exp(i l \varphi) + \exp(-i l \varphi)], \quad (1)$$

where l is the TC of the OAM beam and φ is the azimuthal angle; $k_0 = 2\pi/\lambda$ is the wave number and λ is the wavelength; w_0 is the beam waist of the Gaussian beam, $z_R = \pi w_0^2/\lambda$ is the Rayleigh range and $w(z) = w_0 \sqrt{1 + (z/z_R)^2}$ represents the beam radius.

According to the modified Hill-Andrews spectrum model, the atmosphere refractive index power spectrum can be expressed as¹²

$$\Phi_n(\kappa) = 0.033C_n^2 \frac{\exp(-\kappa^2/\kappa_l^2)}{(\kappa^2 + \kappa_0^2)^{11/6}} \left[1 + 1.802 \left(\frac{\kappa}{\kappa_l} \right) - 0.254 \left(\frac{\kappa}{\kappa_l} \right)^{7/6} \right], \quad (2)$$

where C_n^2 is the refractive index structure constant of atmosphere that describes the strength of atmospheric turbulence; κ is the angular spatial frequency; $\kappa_l = 3.3/l_0$ and $\kappa_0 = 1/L_0$; L_0 and l_0 are the outer and inner scales of atmospheric turbulence, respectively.

The atmospheric turbulence channel is simulated by generating a series of random phase screens.¹³ The random phase screen is related to the refractive index power spectrum as

$$\theta(x, y) = FFT \left[M \sqrt{2\pi k_0^2 \Delta z \Phi_n(\kappa) \cdot [2\pi/(N\Delta L)]^2} \right], \quad (3)$$

where M refers to a complex random matrix with a mean value of 0 and a variance of 1, and FFT refers to the fast Fourier transform. $k_0 = 2\pi/\lambda$ is the wave number, Δz represents the spacing between phase screens, $N \times N$ represents the number of grid points of random phase screens and ΔL represents the grid interval of random phase screens.

The coherence length r_0 can be expressed as the integral of C_n^2 along the propagation path L , which is also related to the wavelength. With the C_n^2 distributed uniformly along the propagation path, the coherence length is¹⁴

$$r_0 = [0.423k^2 C_n^2 L]^{-3/5}. \quad (4)$$

The coherence length r_0 is used to describe turbulence disturbances, which is a measure of the phase distortion of the light wave by turbulence.¹⁵ It is usually measured in centimeters.¹⁶ The typical values of r_0 for turbulence disturbances of whole atmosphere are about 5 cm to 12 cm at visible wavelength,¹⁷ which are included in our simulation. The stronger the turbulence disturbance is, the smaller the value of r_0 is.

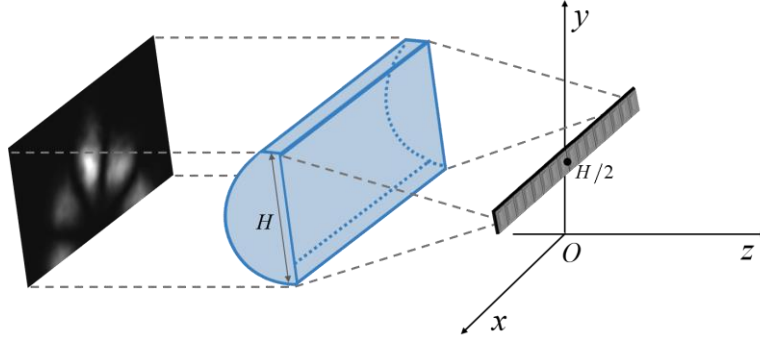


Figure 2. Schematic diagram for the cylindrical lens focusing and 16-unit PDA detection of the superimposed OAM beam.

At the receiver, the OAM beam is focused by two cylindrical lenses and detected by two PDAs. Cylindrical lenses focus light along the y axis only, as shown in Fig. 2. And the transmittance function $t(x, y)$ of the cylindrical lens with a focal length of f can be expressed as¹⁸

$$t(x, y) = \exp \left[-i \frac{k(y - H/2)^2}{2f} \right]. \quad (5)$$

The data are collected to construct datasets to train the CNN for the TC recognition of OAM beams. In terms of the CNN structure, the CNN with a moderate number of layers⁵ is used to balance computational complexity with recognition accuracy. A 1D CNN with a moderate number of layers is proposed for recognition, as shown in Fig. 3.

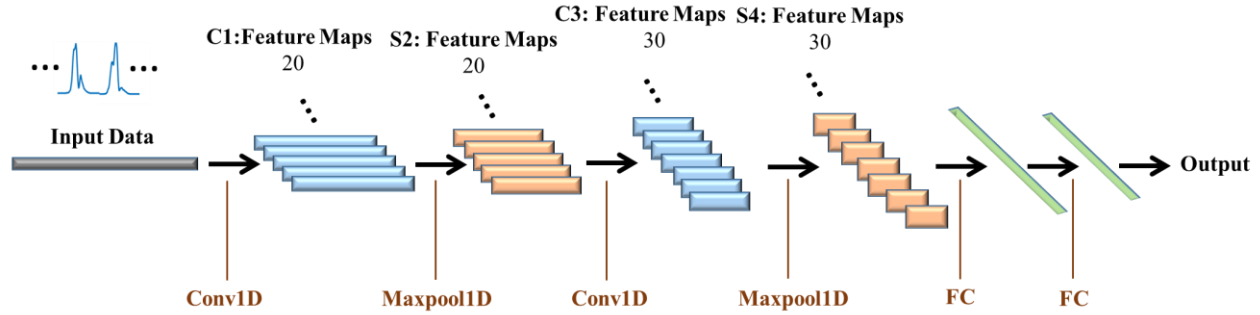


Figure 3. The architecture of the proposed 1D CNN. Conv1D: 1D Convolution operation; Maxpool1D: 1D Max-pooling operation; FC: Fully Connection.

The input data is subjected to two consecutive convolution operations in which filters are convolved with the input to generate feature maps. The two consecutive convolution operations depend on 20 filters of size 3 and stride 1 with no padding. Here, we use two consecutive convolution operations with a small (size 3) filter instead of one convolution operation with a large (size 5) filter to enhance the nonlinear representation of the features and achieve better performance.¹⁹ Immediately, in the max-pooling operation, the original feature maps are down-sampled by calculating the maximum over windows of size 2 to generate 20 feature maps in smaller sizes, where the stride of the windows is 2. Then, under a similar convolution operation and pooling operation, 30 feature maps are activated. After that, all feature maps are successively passed through two fully connected layers. Then a softmax classifier is followed to achieve the classification. We choose rectified linear unit (ReLU) as the activation function and use batch normalizing (BN) for better performance.

2.2 Simulation results

In the simulation, the beam parameters are set to $\lambda = 632.8$ nm (wavelength) and $w_0 = 0.01$ m (waist of the Gaussian beam). The parameter settings for the atmospheric turbulence are as follows: $L_0 = 50$ m (outer scale of atmospheric turbulence), $l_0 = 0.002$ m (inner scale of atmospheric turbulence), $C_n^2 = 5 \times 10^{-16} \sim 5 \times 10^{-15} \text{ m}^{-2/3}$ (the refractive index structure constant of atmosphere), $\Delta z = 200$ m (spacing between phase screens), $N \times N = 512 \times 512$ (grid points of phase screens), and $\Delta L \approx 0.00035$ m (grid interval of phase screens). We simulate a 1 km atmospheric turbulence channel using five random phase screens, as shown in Fig. 4. Turbulence of weak (a 1 km turbulence channel with $C_n^2 = 5 \times 10^{-16} \text{ m}^{-2/3}$, corresponding to the coherence length $r_0 = 16.16$ cm), intermediate (1 km, $C_n^2 = 1 \times 10^{-15} \text{ m}^{-2/3}$, $r_0 = 10.66$ cm) and strong (1 km, $C_n^2 = 5 \times 10^{-15} \text{ m}^{-2/3}$, $r_0 = 4.06$ cm) disturbances are included.

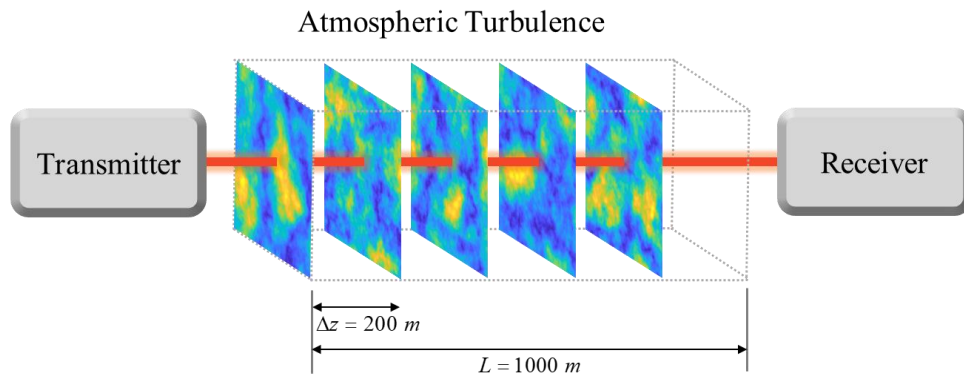


Figure 4. Schematic diagram for simulating a 1 km atmospheric turbulence channel with five random phase screens.

For each superimposed OAM set ($l \in \{\pm 1, \pm 2, \pm 3, \pm 4\}$, $l \in \{\pm 4, \pm 5, \pm 6, \pm 7\}$ and $l \in \{\pm 1, \pm 3, \pm 5, \pm 7\}$), we construct training datasets of mixed turbulence disturbances, including weak ($r_0 = 16.16$ cm), intermediate ($r_0 = 10.66$ cm), and strong ($r_0 = 4.06$ cm) turbulence disturbances. 1600 signals of each TC under turbulence are collected for training and each signal is the connection of two detection signals from two PDAs. The CNN-based

recognition consists of two phases. We first train the CNN of the three superimposed OAM sets and save the best-trained CNN which are later used to recognize the TC of the superimposed OAM beams. Next, the TC recognition performance of the three superimposed OAM sets was investigated under turbulence disturbances varied from weak to strong (the coherence length r_0 is 16.16 cm, 10.66 cm, 7.04 cm, 5.52 cm, 4.64 cm, and 4.06 cm), where 400 test samples are used for each state.

The results of recognition accuracy in the simulation are shown in Fig. 5. The recognition accuracy is defined as the ratio of the number of correctly recognized test samples to the total number of test samples.

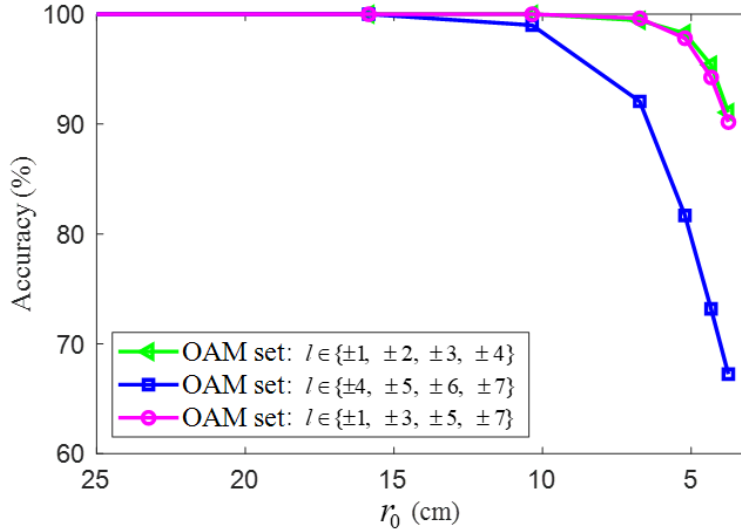


Figure 5. Recognition accuracy of the superimposed OAM sets ($l \in \{\pm 1, \pm 2, \pm 3, \pm 4\}$, $l \in \{\pm 4, \pm 5, \pm 6, \pm 7\}$, and $l \in \{\pm 1, \pm 3, \pm 5, \pm 7\}$) in the simulation.

The simulation results show that the TC recognition accuracy of the superimposed OAM set $l \in \{\pm 1, \pm 2, \pm 3, \pm 4\}$ is 100% under weak (a 1 km turbulence channel with $C_n^2 = 5 \times 10^{-16} \text{ m}^{-2/3}$, corresponding to the coherent length $r_0 = 16.16 \text{ cm}$) and intermediate (1 km, $C_n^2 = 1 \times 10^{-15} \text{ m}^{-2/3}$, $r_0 = 10.66 \text{ cm}$) turbulence disturbances, and 91.06% under a strong (1 km, $C_n^2 = 5 \times 10^{-15} \text{ m}^{-2/3}$, $r_0 = 4.06 \text{ cm}$) turbulence disturbance. The simulation results of the superimposed OAM set $l \in \{\pm 4, \pm 5, \pm 6, \pm 7\}$ under turbulence show that the recognition accuracy decreases when the TC values of superimposed OAM beams increase, limited by the unit number of 16-unit PDAs. The simulation results of the superimposed OAM set $l \in \{\pm 1, \pm 3, \pm 5, \pm 7\}$ can achieve 90.18% accuracy under a strong (1 km, $C_n^2 = 5 \times 10^{-15} \text{ m}^{-2/3}$, $r_0 = 4.06 \text{ cm}$) turbulence disturbance which indicates that the increased TC interval of superimposed OAM beams improves recognition accuracy.

3. EXPERIMENT

3.1 Experimental setup

We conduct an experiment with a 15-m transmission link to further explore the effectiveness of the recognition scheme, as shown in Fig. 6. Four temperature-adjustable hot plates are located about 8 cm under the propagation path, which are about 1 m away from the transmitter, to generate turbulence by convection,²⁰ and each hot plate has an effective area of 10 cm by 10 cm. We adjust the temperature in the range of 100 °C to 300 °C to produce various turbulence disturbances, which can be measured using the angle-of-arrival fluctuations method.¹⁵ The hot plates produce turbulence disturbances with coherence lengths r_0 of 25.31 cm, 17.98 cm, 13.01 cm, 10.18 cm, and 8.59 cm at temperatures of 100 °C, 150 °C, 200 °C, 250 °C, and 300 °C, respectively. Weak ($r_0 = 25.31 \text{ cm}$) to intermediate ($r_0 = 8.59 \text{ cm}$) laboratory-simulated turbulence disturbances are produced.

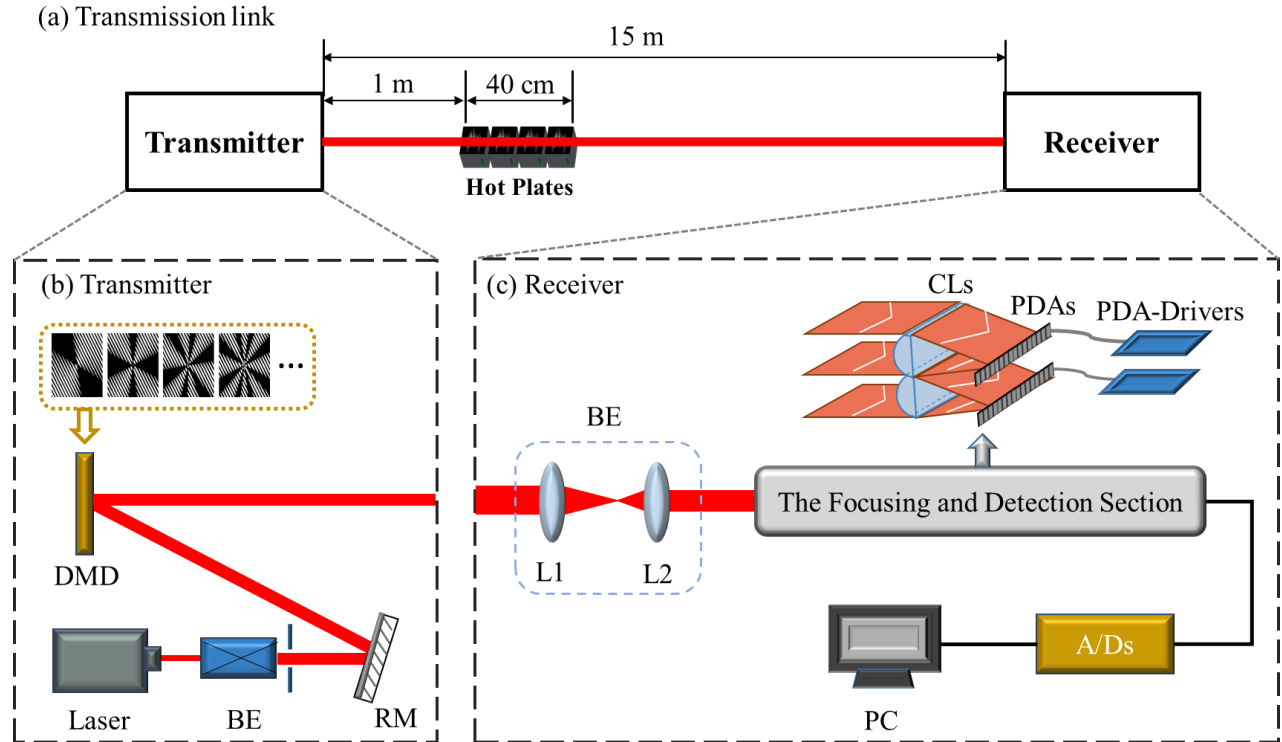


Figure 6. The experimental setup. (a) A 15 m OAM beam transmission link under laboratory-simulated turbulence; (b) Transmitter of OAM beam; (c) Receiver of OAM beam. BE: Beam Expander; RM: Reflecting Mirror; DMD: Digital Micromirror Device; L1, L2: Lenses; CLs: Cylindrical Lenses; PDAs: Photodiode Arrays; A/Ds: Analog-to-Digital Converters.

The OAM beam transmitter is depicted in Fig. 6(b). A beam is emitted by a He-Ne laser (632.8 nm, 2 mW) and then expanded by a beam expander to a diameter of about 3mm. After being reflected by a reflecting mirror, the beam is incident onto a digital micromirror device (DMD), which is loaded with superimposed OAM fork grating maps, to obtain the superimposed OAM beams.

The setup of the OAM beam receiver is shown in Fig. 6(c). The OAM beam, after transmission in turbulence, is first condensed in a ratio of 3:1 to a suitable size to fit the size of cylindrical lenses. Then, the beam is focused by two 20-mm-by-20-mm cylindrical lenses with a focal length of 75 mm and detected by two PDAs. The PDA (S4111-16Q, Hamamatsu Co.) consists of 16 units. The photosensitive area of the unit is 1.45 mm by 0.9 mm, and the spacing between units is 0.1 mm. The analog signals measured by the detection section are then converted to digital signals by the A/Ds (16 bits, 200 kSPS). The data are used as input to the CNN for eventual recognition.

In the experiment, we construct training datasets under mixed laboratory-simulated disturbances (the coherence length r_0 is 25.31 cm, 17.98 cm, 13.01 cm, 10.18 cm, and 8.59 cm) for each of the three superimposed OAM sets ($l \in \{\pm 1, \pm 2, \pm 3, \pm 4\}$, $l \in \{\pm 4, \pm 5, \pm 6, \pm 7\}$ and $l \in \{\pm 1, \pm 3, \pm 5, \pm 7\}$). 1600 signals of each TC under turbulence are collected for training, and each signal is the connection of two detection signals from two PDAs. The CNN-based recognition consists of two phases. First, we train the CNN of the three superimposed OAM sets and save the best-trained CNN for each, which are subsequently used to recognize the TC of superimposed OAM beams. Next, the real-time TC recognition performance of each of the three superimposed OAM sets under the laboratory-simulated turbulence disturbances was investigated, where 1000 test samples are used for each state.

3.2 Experimental results

The experimental results on recognition accuracy are shown in Fig. 7, where the recognition accuracy is defined as the ratio of the number of correctly recognized test samples to the total number of test samples.

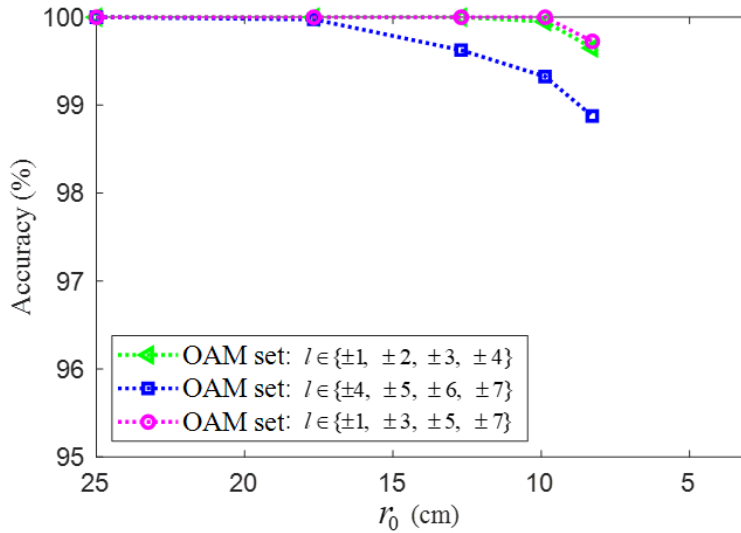


Figure 7. Recognition accuracy of the superimposed OAM sets ($l \in \{\pm 1, \pm 2, \pm 3, \pm 4\}$, $l \in \{\pm 4, \pm 5, \pm 6, \pm 7\}$, and $l \in \{\pm 1, \pm 3, \pm 5, \pm 7\}$) in the experiment.

Experimentally, the accuracy of the superimposed OAM set $l \in \{\pm 1, \pm 2, \pm 3, \pm 4\}$ is 100% and 99.65% under weak ($r_0 = 25.31 \text{ cm} \sim 13.01 \text{ cm}$) and intermediate ($r_0 = 8.59 \text{ cm}$) turbulence-simulated disturbances, respectively. The experimental results of the superimposed OAM set $l \in \{\pm 4, \pm 5, \pm 6, \pm 7\}$ under weak and intermediate turbulence-simulated disturbances verify that the recognition accuracy decreases as the TC values of superimposed OAM beams increase. The experimental results of the superimposed OAM set $l \in \{\pm 1, \pm 3, \pm 5, \pm 7\}$ under weak and intermediate turbulence-simulated disturbances also verify that increasing the TC interval of superimposed OAM beams improves accuracy.

In terms of the recognition rate in our experimental system, due to the use of PDAs, it mainly depends on the inference time of the CNN. And the inference time of the proposed CNN on an i7-8750H CPU is about 0.5 ms, which can be further accelerated by the hardware.

4. CONCLUSION

In conclusion, a new CNN-based scheme using linear photodiode array detectors for recognizing the TC of superimposed OAM beams is proposed and investigated. Both simulation and experimental results verify the feasibility and effectiveness of the proposed scheme. The effects of the atmospheric turbulence disturbances, the TC values of superimposed OAM beams, and the TC intervals of superimposed OAM beams on the recognition accuracy in the proposed scheme are explored. These results may have positive implications for the application of the OAM-FSO communication.

REFERENCES

- [1] Wang, J., Yang, J. Y., Fazal, I. M., Ahmed, N., Yan, Y., Huang, H., Ren, Y., Yue, Y., Dolinar, S., Tur, M., and Willner, A. E., "Terabit free-space data transmission employing orbital angular momentum multiplexing," *Nat. Photonics* 6(7), 488-496 (2012).
- [2] Liu, Z., Yan, S., Liu, H., and Chen, X., "Superhigh-resolution recognition of optical vortex modes assisted by a deep-learning method," *Phys. Rev. Lett.* 123(18), 183902 (2019).
- [3] Zhu, X. and Kahn, J. M., "Free-space optical communication through atmospheric turbulence channels," *IEEE Trans Commun* 50(8), 1293-1300 (2002).

- [4] Liu, J., Wang, P., Zhang, X., He, Y., Zhou, X., Ye, H., Li, Y., Xu, S., Chen, S., and Fan, D., "Deep learning based atmospheric turbulence compensation for orbital angular momentum beam distortion and communication," *Opt. Express* 27(12), 16671-16688 (2019).
- [5] Lohani, S., Knutson, E. M., O'Donnell, M., Huver, S. D., and Glasser, R. T., "On the use of deep neural networks in optical communications," *Appl. Opt.* 57(15), 4180-4190 (2018).
- [6] Krenn, M., Fickler, R., Fink, M., Handsteiner, J., Malik, M., Scheidl, T., Ursin, R., and Zeilinger, A., "Communication with spatially modulated light through turbulent air across Vienna," *New J. Phys* 16(11), 113028 (2014).
- [7] Li, J., Zhang, M., and Wang, D., "Adaptive demodulator using machine learning for orbital angular momentum shift keying," *IEEE Photon. Technol. Lett.* 29(17), 1455-1458 (2017).
- [8] Li, J., Zhang, M., Wang, D., Wu, S., and Zhan, Y., "Joint atmospheric turbulence detection and adaptive demodulation technique using the CNN for the OAM-FSO communication," *Opt. Express* 26(8), 10494-10508 (2018).
- [9] Wang, J. and Zhu, B., "A new scheme using convolutional neural network to recognize orbital angular momentum beams disturbed by atmospheric turbulence," *ACP/IPOC 2020 - Proceedings*, M4A.310 (2020).
- [10] Cui, X., Yin, X., Chang, H., Guo, Y., Zheng, Z., Sun, Z, Liu, G., and Wang, Y., "Analysis of an adaptive orbital angular momentum shift keying decoder based on machine learning under oceanic turbulence channels," *Opt. Commun.* 429, 138-143 (2018).
- [11] Yuan, Y., Lei, T., Gao, S., Weng, X., Du, L., and Yuan, X., "The orbital angular momentum spreading for cylindrical vector beams in turbulent atmosphere," *IEEE Photon. J.* 9(2), 1-10 (2017).
- [12] Andrews, L. C. and Phillips, R. L., [*Laser beam propagation through random media*], SPIE, Bellingham, 57-82 (2005).
- [13] Lochab, P., Senthilkumaran, P., and Khare, K., "Propagation of converging polarization singular beams through atmospheric turbulence," *Appl. Opt.* 58(23), 6335-6345 (2019).
- [14] Li, S., Chen, S., Gao, C., Willner, A. E., and Wang, J., "Atmospheric turbulence compensation in orbital angular momentum communications: Advances and perspectives," *Opt. Commun.* 408, 68-81 (2018).
- [15] Novoseller, D. E., "Coherence length evaluation for linear propagation of radiation through a turbulent medium," *Appl. Opt.* 19(3), 352-354 (1980).
- [16] Tunick, A., "Optical turbulence parameters characterized via optical measurements over a 2.33 km free-space laser path," *Opt. Express* 16(19), 14645-14654 (2008).
- [17] Qiang, X., Li, Y., Zong, F., and Zhao, J., "Measurement of laboratory-simulated atmospheric turbulence by PSD," *ICEMI' 2009 - Proceedings*, 2-90-2-94 (2009).
- [18] Goodman, J. W., [*Introduction to Fourier Optics*], McGraw-Hill, New York, 269 (1996).
- [19] Simonyan, K. and Zisserman, A., "Very deep convolutional networks for large-scale image recognition," *arXiv preprint arXiv:1409.1556* (2014).
- [20] Anguita, J. A. and Cisternas, J. E., "Influence of turbulence strength on temporal correlation of scintillation," *Opt. Lett.* 36(9), 1725-1727 (2011).